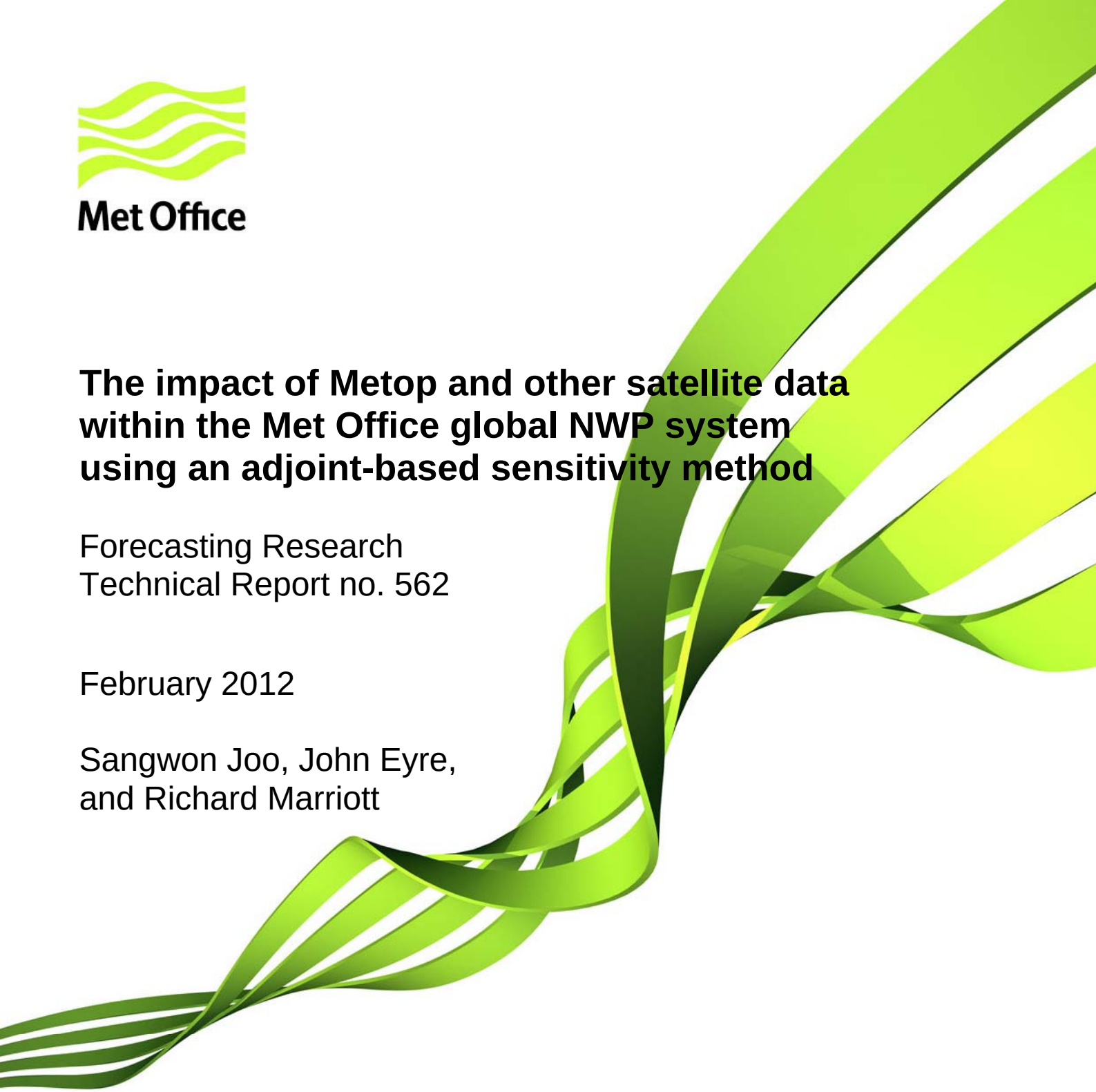

The impact of Metop and other satellite data within the Met Office global NWP system using an adjoint-based sensitivity method

Forecasting Research
Technical Report no. 562

February 2012

Sangwon Joo, John Eyre,
and Richard Marriott

Contents

Abstract

Observation impacts on 24-hour forecast error reduction are evaluated using the adjoint-based Forecast Sensitivity to Observations (FSO) method developed within the Met Office NWP system. The observation impacts of various subsets of observations are compared, with emphasis on space-based observations, particularly those from instruments on-board the Metop-A platform.

Satellite data are found to account for 64% of short-range global forecast error reduction, the remaining 36% being due to the assimilation of surface-based observation types. Metop-A data are measured as having the largest impact of any individual satellite platform (about 25% of the total impact on global forecast error reduction). Their large impact, compared to that of NOAA satellites, is mainly due to Metop's additional sensors (IASI, ASCAT and GRAS). Microwave and hyper-spectral IR sounding techniques are found to give the largest total impacts; however, the GPSRO technique was measured as having the largest observation impact per sounding.

This study has demonstrated how the FSO technique can be used to assess the impact of satellite data types in NWP. This information can be used to guide improvement of the use of currently available data and to contribute to discussions on the evolution of future observing systems.

1. Introduction

The contribution of satellite data to the accuracy of global NWP now exceeds that of surface-based observations. This has been achieved mainly through better usage of satellite data within the data assimilation process (Bouttier and Kelly, 2001; Kelly and Thépaut, 2007; Gelaro et al., 2010). The Met Office is continually working to expand the range of satellite data assimilated, in order to improve NWP accuracy. Most recently, data from the IASI instrument on-board Metop-A have been assimilated over land, through better specification of the surface emissivity (Pavelin et al., 2012).

The impacts of newly available satellite data or improved assimilation methods are traditionally tested in "Observing System Experiments" (OSEs) or "data-denial" experiments, through which the impact of the new data/methods is evaluated through comparison of forecast output with that of a "control run" which usually comes from the

current operational NWP system. In this way, the contribution of each development can be assessed one by one; however, using such methods, it is not easy to assess the relative contributions of each assimilated satellite data-type to forecast accuracy at any given time; this would involve an exhaustive set of OSEs in which each satellite data-type is excluded in turn. As a consequence, the relative impact of satellite data-types within the Met Office global NWP system has not recently been evaluated in a systematic way. Nevertheless, such evaluations are useful for checking the impact of each satellite data type as the system evolves: Impacts may have been beneficial when the data-types were first introduced, but are they now? Also such evaluations can make an important contribution to discussions on the evolution and design of future observation systems. At the present time, it is particularly important to understand the impact of data from the Metop-A satellite in order to guide preparations for the next generation of European polar orbiting satellites.

In order to evaluate the relative impact of each observation type, the adjoint-based Forecast Sensitivity to Observations (FSO) method developed for the Met Office global NWP system has been used (Lorenc and Marriott, 2012). The system estimates a forecast impact for each piece of observational information assimilated. All impacts are produced simultaneously and so the method is efficient. Impacts can be easily aggregated making the method extremely useful for evaluating the impact of satellite data, which consists of many sub-types. The impact of each of these sub-types cannot be regularly assessed in an affordable manner through the use of OSEs alone.

The purpose of this report is to document an evaluation of the relative impact of satellite data in the Met Office global NWP system, and so to inform discussions on future satellite systems. A brief introduction to the adjoint-based method, a summary of satellite data usage at the Met Office and a description of the experimental design are given in section 2. The results and their discussion are given in section 3 and 4, with a summary and comments on future work in section 5.

2. Method

2a. The Forecast Sensitivity to Observations (FSO) method

This study utilises an adjoint-based Forecast Sensitivity to Observations (FSO) method similar to that originally developed in Langland and Baker (2004). Our method is subtly different from that in Langland and Baker (2004) in ways which will be stressed in this

section. Full details of the Met Office system are documented in Lorenc and Marriott (2012).

We are using the Met Office FSO system to measure the impact of observations on global 24-hour forecast error. The adjoint method requires that forecast error be represented by a single scalar value. We choose to do this by using a global total energy norm,

$$J = (\delta \mathbf{w}^f)^T \mathbf{C} (\delta \mathbf{w}^f) , \quad (1)$$

where $\delta \mathbf{w}^f$ represents the "error" in a simplified global forecast state (as given by the difference from a verifying analysis, which is assumed to be independent of that used to initialise the forecast in question); superscript T denotes the transpose operator; and $\mathbf{C}$ is a diagonal inner-product matrix of energy weights with non-zero elements corresponding to values of horizontal wind, temperature, pressure and humidity. Weights corresponding to gridpoints above 150 hPa are set to zero. The forecast impact is then the change in this total energy as a result of assimilating a batch of observations (usually negative corresponding to a reduction in forecast error). This is given by

$$\delta J = (\delta \mathbf{w}_t^{fa})^T \mathbf{C} (\delta \mathbf{w}_t^{fa}) - (\delta \mathbf{w}_t^{fb})^T \mathbf{C} (\delta \mathbf{w}_t^{fb}) \quad (2)$$

where $\delta \mathbf{w}_t^{fa}$ is the error in a simplified forecast state initialised from an analysis and $\delta \mathbf{w}_t^{fb}$ is that initialised from the background state of that analysis. (Both forecast states are valid at time t and are verified against the same analysis.) As (2) is the difference of two squares it can be written as

$$\delta J = (\delta \mathbf{w}_t)^T \mathbf{C} (\delta \mathbf{w}_t^{fa} + \delta \mathbf{w}_t^{fb}) = (\delta \mathbf{w}_t)^T \left(\frac{\delta J}{\delta \mathbf{w}_t} \right) \quad (3)$$

where $\delta \mathbf{w}_t = (\delta \mathbf{w}_t^{fa} - \delta \mathbf{w}_t^{fb})$ is also equivalent to the change in forecast state due to the assimilation of observations. We will call $\left(\frac{\delta J}{\delta \mathbf{w}_t} \right) = \mathbf{C} (\delta \mathbf{w}_t^{fa} + \delta \mathbf{w}_t^{fb})$ the forecast sensitivity vector, which can be thought of as the finite gradient in an exact linear expression for the impact of $\delta \mathbf{w}_t$ on δJ (conceding the fact that it is, itself, dependent on $\delta \mathbf{w}_t$). Note that the forecast sensitivity vector is equivalent to the average of the gradients of (1) at the points of the forecast from analysis and the forecast from background. In Langland and Baker (2004), linearisation errors are taken account of by a similar averaging of gradients, but at the analysis time rather than the forecast time. By averaging at the forecast time we take account of the quadratic nature of (1), which is the dominant nonlinearity of the FSO problem (Gelaro, Zhu and Errico, 2007), and we are left with only a single forecast sensitivity vector to which we need only apply the adjoint forecast model once, as shown in the following.

Our goal is not to express the impact, δJ, in terms of the change in forecast state, $\delta \mathbf{w}_t$, but to express it in terms of observation innovations (the difference of observations from the NWP background estimate). We note that the change in forecast state is due to the assimilation of observations and can be approximated by the expression

$$\delta \mathbf{w}_t \approx \mathbf{MK}\delta \mathbf{y} \quad (4)$$

where $\delta \mathbf{y}$ is the vector of observation innovations; $\mathbf{K}$ is the Kalman gain matrix implicitly calculated by our incremental four-dimensional variational (4D-Var) data assimilation scheme; and $\mathbf{M}$ is the linearised version of our forecast model, the normal use of which is as part of 4D-Var. (4) is only an approximation as, in reality, neither $\mathbf{K}$ nor $\mathbf{M}$ is linear: nonlinearities in $\mathbf{K}$ are small and can be ignored but in $\mathbf{M}$ they are larger and can lead to significant linearisation error (Lorenc and Marriott, 2012). Other reasons for non-equivalence in (4) are that $\mathbf{M}$ operates on simplified model states and uses simplified physics schemes.

Substituting (4) into (3) we get

$$\delta J \approx (\mathbf{MK}\delta \mathbf{y})^T \left(\frac{\delta J}{\delta \mathbf{w}_t} \right) = \delta \mathbf{y}^T \mathbf{K}^T \mathbf{M}^T \mathbf{C}(\delta \mathbf{w}_t^{fa} + \delta \mathbf{w}_t^{fb}) \quad (5)$$

$$\left(\frac{\delta J}{\delta \mathbf{y}} \right) \approx \mathbf{K}^T \mathbf{M}^T \mathbf{C}(\delta \mathbf{w}_t^{fa} + \delta \mathbf{w}_t^{fb}) \quad (6)$$

where (6) is our vector of "finite observation sensitivities" and $\mathbf{M}^T$ and $\mathbf{K}^T$ are the adjoint forecast model and adjoint data assimilation scheme, respectively. The adjoint forecast model is available as a standard component of our variational data assimilation system. To mitigate against the linearisation problems mentioned with reference to (4), $\mathbf{M}^T$ is linearised about the forecast trajectory which is the average of those initialised from background and analysis states (Lorenc and Marriott, 2012). While $\mathbf{M}^T$ is a line-by-line adjoint, $\mathbf{K}^T$ is applied by utilising a modified version of Met Office 4D-Var, making use of existing software to minimise a modified cost-function. $\mathbf{K}^T$ is, therefore, only the adjoint of $\mathbf{K}$ when full convergence is reached. Our 4D-Var allows the observation operators, and hence the Kalman gain, $\mathbf{K}$, to be weakly nonlinear. The adjoint is only defined for a linear operator; we choose to linearise $\mathbf{K}$ about the final analysis (Lorenc and Marriott, 2012).

(6) is a vector which contains a sensitivity corresponding to each observation in $\delta \mathbf{y}$. An estimate of the contribution to the total impact of the kth observation is given by

$$\delta J_k \approx \delta y_k \left(\frac{\delta J}{\delta \mathbf{y}} \right)_k . \quad (7)$$

Note though that, as previously mentioned, the vector of sensitivities contains dependencies on $\delta \mathbf{y}$. The application of $\mathbf{MK}$ to observation innovations in (4) and the fact that (4) is present in the forecast sensitivity vector mean that (7) contains cross-products with many elements of $\delta \mathbf{y}$, i.e. the impact of observation k cannot be uniquely untangled from the total impact. This is a consequence of using (1) at the analysis point, which is nonlinear in $\delta \mathbf{y}$, in (3) to obtain an exact expression for the total impact. Gelaro, Zhu and Errico (2007) shows that contributions to partial impacts from cross-products with observation innovations outside the set in question are dominated by linear contributions from within the set itself, at least for fairly large sets of observations. We therefore use (7) to calculate impacts for subsets of observations, making the assumption that the influence of observations external to that set is small and that all subsets are affected in a similar way such that relative impacts are not affected.

2b. Satellite data usage

Satellite instruments do not, in general, observe the NWP analysis variables directly; satellite observations are compared with analysis variables via "observation operators" within a data assimilation system. Nevertheless, each satellite data-type is affected by, and provides information on, a limited number of analysis variables. The satellite observation types used in this study, and the NWP variables about which these observations contain most information, are listed at Table 1.

Table 1. Satellite observation types used in this study and affected NWP variables

Observation Type	Satellite	NWP Variables
AMSU/MHS radiances	4 NOAA (15,17,18,19) + Metop-A	Temperature, humidity
HIRS clear radiances	2 NOAA (17,19)+ Metop-A	Temperature, humidity
IASI and AIRS clear,cloudy radiances	Metop-A + Aqua	Temperature, humidity
SSMIS radiances	DMSP(F16)	Temperature, humidity
Geo imager clear IR radiances	MSG(Meteosat-9) , GOES	Humidity
GPS RO bending angles	5 COSMIC, Metop-A/GRAS, GRACE-A	Temperature, humidity
AMVs-GEO	Meteosat-7, MSG(Meteosat-9), MTSAT, GOES-11, GOES-13	Wind
SEVIRI Clear sky radiances	MSG(Meteosat9)	Temperature, humidity
AMVs-MODIS and AVHRR	Aqua, Terra, NOAA	Wind
Scatterometer sea-surface wind	Metop-A/ASCAT	Surface wind
MW imager sea-surface wind	Coriolis/WINDSAT	Surface wind
Cloud-top height / amount	MSG/SEVIRI	Cloud
SSTs: AVHRR, AATSR	NOAA, Metop-A, ENVISAT, Aqua	Sea surface temperature
Soil Moisture: ASCAT	Metop-A	Soil moisture
Sea ice: SSMI, SSMIS	DMSP	Sea ice
Snow cover	Various	Snow cover

Note that some of these NWP variables – SST, sea-ice, snow cover and soil moisture – are initialised separately, and not as part of the 4D-Var process. Consequently, the impact of observations important for their analysis will not be measured by the FSO method.

2c. Experimental design

The global NWP system used for this experiment is the system used operationally at the Met Office from 16 March 2011 (referred to internally as parallel suite 26, PS26). The analyses are produced using 4D-Var with a 6-hour cycle. The horizontal resolution

of the nonlinear forecast model is N320 (about 40km), with 70 vertical levels up to 60km. The linear model in 4D-Var includes moist processes and has the same vertical resolution as the non-linear model with a horizontal resolution of N216 (about 60km).

Observation impacts give an estimate of the change in 24-hour forecast error due to the assimilation of observations. Forecast error is measured using a global moist energy norm extending from the surface to 150 hPa as described in section 2a. The total forecast impact is approximated by a global sum of the observation impact which will be called the “total observation impact” hereafter. The term ”observation impact” will refer to partial sums of observation impact over various subsets unless otherwise specified. Observation impact can be used to assess the relative importance of each observation type in the context of this experiment; however, because observation impact depends on the data-accumulation period, it should not be compared directly with that of experiments looking at different periods. It is more appropriate to compare the mean impact per observation, hereafter known as the “mean observation impact”.

The observation impacts are produced for the period from 18Z 22 August to 12Z 18 September 2010 in 6-hour intervals. These times are nominal analysis times, with observation spread within +/- 3 hours. A few analyses are not used in calculating the observation impact because the impacts are exaggerated due to computational stability problems, as discussed by Joo et al. (2012). The data period, the impact measure and the NWP system used for this experiment are summarized in Table 2.

Table 2. Summary of experiment

Data period	From 18Z 22 August to 12Z 18 September 2010, except 18Z 30 Aug and 00,06,12Z 5 September 2010
Impact Measure	24-hour forecast error reduction of global moist energy norm from surface to 150hPa
NWP system	Operational version of Met Office global NWP system at 16 March 2011 (PS26), with the resolution of N320 for UM and N216 for inner loop of 4D-Var in horizontal, and 70 levels in vertical. The adjoint of PF model used in this experiment is run with moist physics.

The impact of Metop-A and other satellite data are evaluated using 5 subsets as follows. The details of data used for each subset are listed in Table 3.

- Metop impact: The impact of Metop-A data, compared with the impacts of observations from other satellites and of surface-based observations.
- Per platform: The impact of data from each satellite platform.
- Per technique: The impact of data from each satellite observing technique: MWS (microwave soundings), IRS (infra-red soundings), SCAT (scatterometry), GPSRO (GPS radio occultation), Imager/AMV (atmospheric motion vectors derived from visible/infra-red imagery), and MWI (Microwave imagery).
- Metop sensor : The impact of data from each sensor on-board Metop-A.
- Operational/Research: The impact of data from operational and research satellites.

It is should be noted that the “SONDE” sub-type in Table 3 includes the impact of wind profilers, and that the SFC LAND sub-type includes “BOGUS” data. This does not

affect the conclusions because the wind profiler and BOGUS impacts are almost negligible in this study.

It should also be noted that the SSMIS channels used in this study (channels 2-11, 9-16, 21-23) give these data the characteristics of a SSMI-like microwave imager and an AMSU-A/MHS-like microwave sounder. There is also additional temperature sounding capability in the upper stratosphere and mesosphere, but the impact of these channels will not be measured by the FSO technique with a tropospheric energy norm. Because of the relatively low impact of SSMIS and for simplicity, it has been categorised as "MWI" for the purposes of this study.

Table 3. Detailed observations for each subset compared.

Subset name / Observation	Sub-type	Platform	Technique	Metop sensor	Operational /Research
Metop-A/IASI	Metop	Metop-A	IRS	IASI	Operational
Metop-A/AMSU-A	Metop	Metop-A	MWS	AMSU-A	Operational
Metop-A/MHS	Metop	Metop-A	MWS	MHS	Operational
Metop-A/HIRS	Metop	Metop-A	IRS	HIRS	Operational
Metop-A/ASCAT	Metop	Metop-A	SCAT	ASCAT	Operational
Metop-A/GRAS	GPSRO	Metop-A	GPSRO	GRAS	Research
NOAA-15/AMSU-A	NOAA	NOAA-15	MWS	N/A	Operational
NOAA-15/AVHRR	NOAA	NOAA-15	Imager/AMV	N/A	Operational
NOAA-16/AVHRR	NOAA	NOAA-16	Imager/AMV	N/A	Operational
NOAA-17/HIRS	NOAA	NOAA-17	IRS	N/A	Operational
NOAA-17/AVHRR	NOAA	NOAA-17	Imager/AMV	N/A	Operational
NOAA-18/AMSU-A	NOAA	NOAA-18	MWS	N/A	Operational
NOAA-18/MHS	NOAA	NOAA-18	MWS	N/A	Operational
NOAA-18/AVHRR	NOAA	NOAA-18	Imager/AMV	N/A	Operational
NOAA-19/HIRS	NOAA	NOAA-19	IRS	N/A	Operational
NOAA-19/AMSU-A	NOAA	NOAA-19	MWS	N/A	Operational
NOAA-19/AVHRR	NOAA	NOAA-19	Imager/AMV	N/A	Operational
EOS-Aqua/AIRS	Other LEO	Aqua	IRS	N/A	Research
EOS-Aqua/MODIS	Other LEO	Aqua	Imager/AMV	N/A	Research
EOS-Terra/MODIS	Other LEO	Terra	Imager/AMV	N/A	Research
DMSP F-16/SSMIS	Other LEO	DMSP F-16	MWI	N/A	Operational
ERS2/AMI	Other LEO	ERS-2	SCAT	N/A	Research
Coriolis/WindSat	Other LEO	Coriolis	MWI	N/A	Research
GOES/AMVs	GEO	GOES	Imager/AMV	N/A	Operational
MTSAT/AMVs	GEO	MTSAT	Imager/AMV	N/A	Operational
Meteosat/AMVs	GEO	Meteosat	Imager/AMV	N/A	Operational
Meteosat/SEVIRI CLR	GEO	Meteosat	Imager/AMV	N/A	Operational
COSMIC	GPSRO	Other RO	GPSRO	N/A	Research
GRACE	GPSRO	Other RO	GPSRO	N/A	Research
AMDAR	AIRCRAFT	N/A	N/A	N/A	N/A
AIREP	AIRCRAFT	N/A	N/A	N/A	N/A

PILOT	“SONDE”	N/A	N/A	N/A	N/A
TEMP	“SONDE”	N/A	N/A	N/A	N/A
DROP SONDE	“SONDE”	N/A	N/A	N/A	N/A
Wind Profiler	“SONDE”	N/A	N/A	N/A	N/A
SYNOP	SFC LAND	N/A	N/A	N/A	N/A
BOGUS	SFC LAND	N/A	N/A	N/A	N/A
TCBOGUS	SFC SEA	N/A	N/A	N/A	N/A
BUOY	SFC SEA	N/A	N/A	N/A	N/A
SHIP	SFC SEA	N/A	N/A	N/A	N/A

3. Results

3a. Observation Impact by “Sub-type”

Figure 1 shows the observation impact of the observation subsets described by the “Sub-type” column of Table 3. Of all the observation categories, Metop has the largest impact on global forecast error reduction, and its contribution in reducing the short-range forecast error is about 25% of the total observation impact of all assimilated observations (Figure 1). The observation impact of satellite data dominates the surface-based observations; about 64% of the short-range forecast-error reduction is due to satellite observations and the other 36% to surface-based observations. The ranking of sub-types by observation impact is led by “SONDE” (15%), followed by aircraft (9%), land surface (7%) and sea surface data (5%). The observation impact of satellite is mainly led by LEOs, including Metop and NOAA. LEOs contribute about 58% of the total observation impact on short-range NWP forecast-error, whilst GEOs contribute only about 6%.

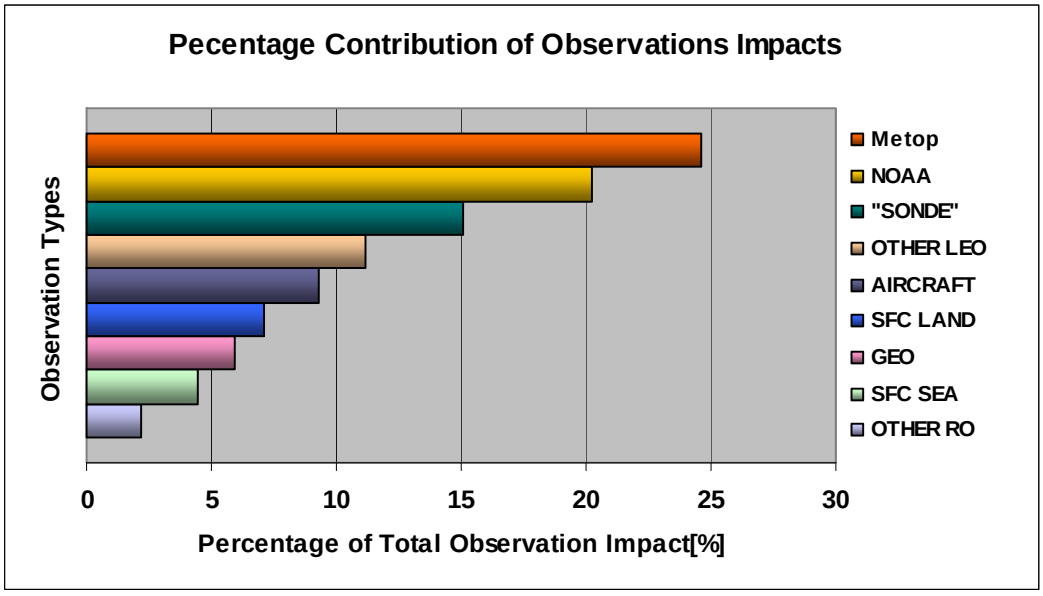

Figure 1. Comparison of the observation impact of Metop with other observation types as specified by the “sub-type” column of Table 3. The fraction of the total observation impact is expressed as a percentage.

3b. Observation impact by "Platform"

The observation impact of each satellite platform is evaluated and the results are shown in Figure 2. Metop-A is measured as having the largest impact of any satellite platform (38% of the observation impact of all satellite platform), followed by NOAA and Aqua. The observation impact of NOAA-16 is negligible because only AVHRR AMVs are assimilated during the period of this experiment (see Table 1). Meteosat shows the strongest impact among GEO satellites, its impact here being mainly due to AMVs; the SEVIRI clear-sky radiance (CLR) impact is an order of magnitude lower than the AMV impact.

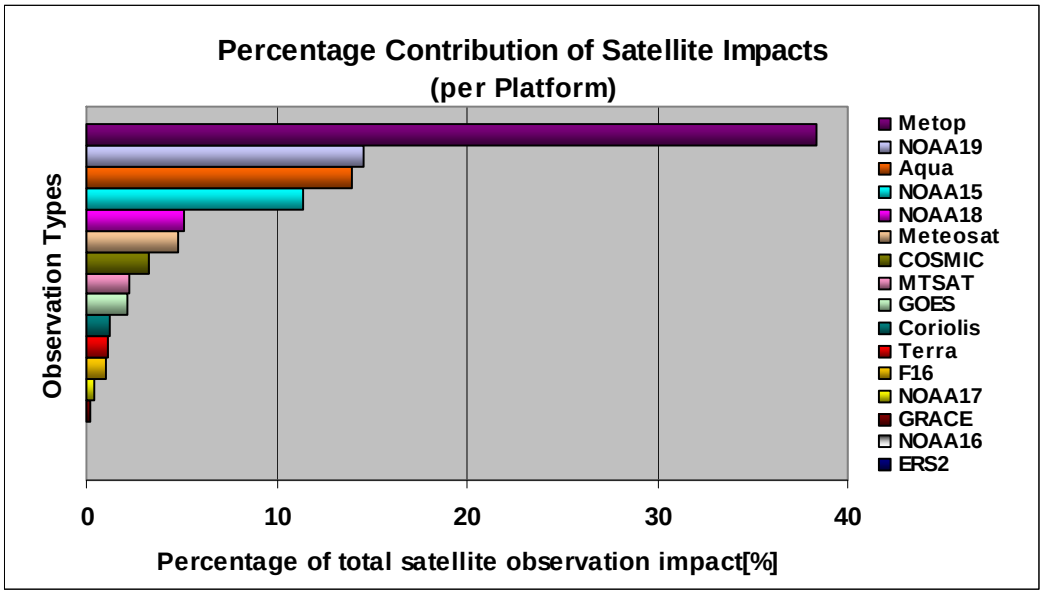

Figure 2. As in Figure 1, but for the "platform" categories described in Table 3. The fraction of the total satellite observation impact is expressed as a percentage.

The observation impact and mean observation impact of AMVs are shown in Figure 3 to check whether the large observation impact of the Meteosat (compared with some other GEOs) is due to the large observation numbers or to the large impact of each individual observation. The observation impact of MSG (Meteosat 9) and MTSAT are larger than for the other GEO satellites, and NOAA AVHRR shows a very small impact (Figure 3a) while the mean observation impacts are quite similar to each other (Figure 3b). It can be inferred that number of observations is the main factor in differentiating the AMV impact of each platform in the Met Office global NWP system.

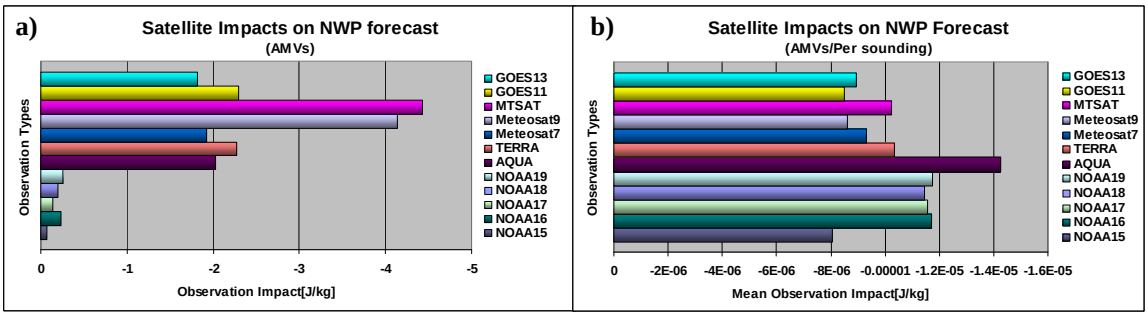

Figure 3. The AMV impact on the forecast error reduction between platforms. a) and b) show observation impact and mean observation impact respectively.

3c. Observation impact by "Technique"

Observation impact of satellite by technique is shown in Figure 4. The microwave and infra-red sounders together are measured as having an impact of about 79% of the observation impact of all satellite; 45% is from microwave soundings and the other 34% from infra-red soundings. The imagers account for 11%, followed by scatterometers (5%) and GPSRO (4%) (Figure 4a). By contrast, GPSRO data give the largest mean observation impact (Figure 4b).

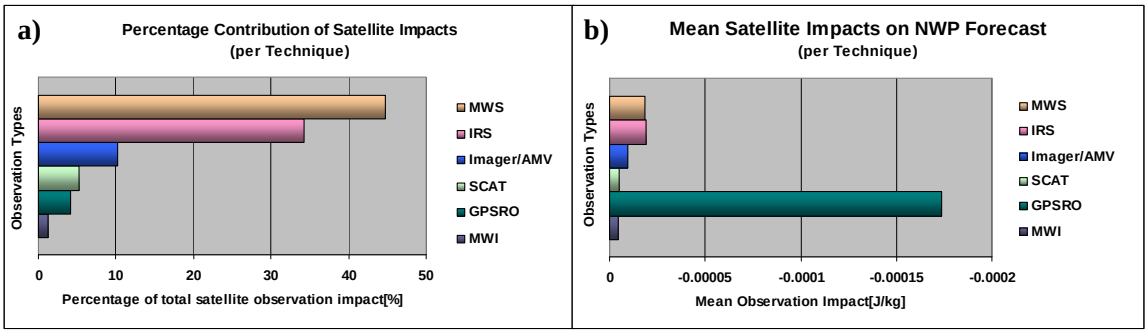

Figure 4. Comparison of the impacts from observations of each satellite observing technique as described by the "technique" column of Table 3. a) and b) show observation impact and mean observation impact respectively.

In Figure 4, the IRS instruments show a smaller impact than the MWS instruments; however, it is necessary to distinguish between the more modern hyper-spectral infra-red sounders (IASI and AIRS) and the older instruments, such as HIRS. Figure 5 shows the observation impact and mean observation impact of each sounder in this study. The impacts per sounding of the hyper-spectral IR sounders, Metop-A/IASI and Aqua/AIRS, are larger than those of the microwave sounders. The observation impact of NOAA-18/AMSU-A is smaller than the other AMSU-As because the number of soundings used is less for NOAA-18 than for the others.

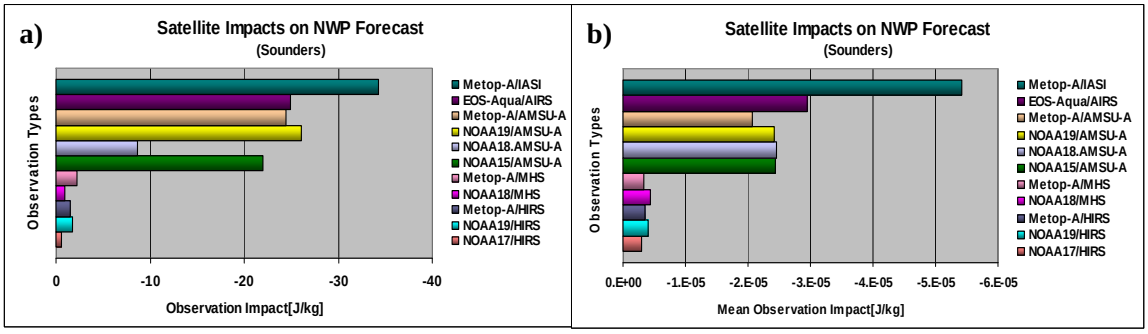

Figure 5. a) Observation impacts and b) mean observation impacts of the instruments using MWS and IRS techniques.

3d. Observation impact for "Operational/Research" subsets

Figure 6 compares the impact of operational satellite data to that of research satellite data. In terms of observation impact, that of operational satellites is four times larger than that of research satellites. In contrast, research satellites have a larger impact per

sounding than operational satellites. Most of the contribution of research satellites is from Aqua/AIRS, as was shown in Figures 2 and 5.

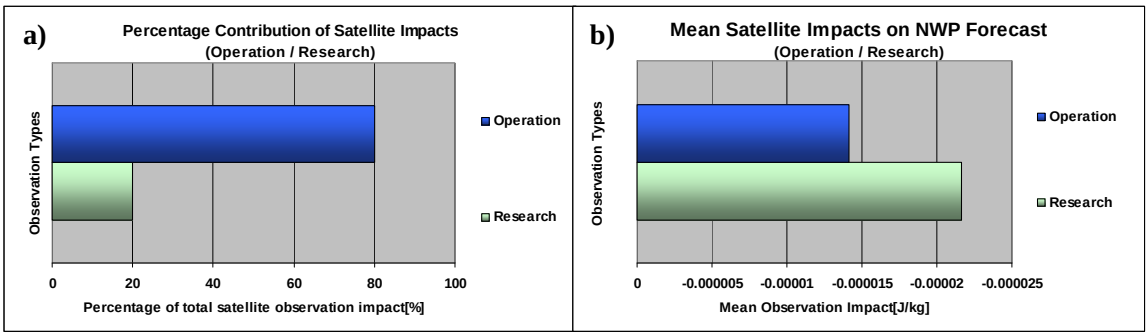

Figure 6. As in Figure 4, but for the ”Operational/Research” subsets described in Table 3.

3e. Observation impact for Metop sensors

The impact of each sensor on-board Metop-A is compared in Figure 7. IASI is the most valuable sensor on Metop-A, giving about 46% of the observation impact of Metop-A , followed by AMSU-A (33%), ASCAT(14%), MHS(3%), GRAS(2%) and HIRS(2%). The relatively small observation impacts of HIRS and MHS are also seen in equivalent plots for NOAA series satellites (not shown here). The observation impacts of AMSU-A, MHS and HIRS on-board Metop-A are similar to those for NOAA satellites, as was shown in Figure 5a. The dominant role of Metop-A in reducing the forecast error, compared with the NOAA series satellites, is mainly due to the additional instruments - IASI, ASCAT and GRAS.

GRAS shows the largest mean observation impact; however, comparing Figure 7 with Figure 4b, GRAS data are shown to have a smaller impact than other GPSRO data. This is partly because GRAS data are not yet used below 10km, where GPSRO shows strong positive impact (Cardinali, 2009).

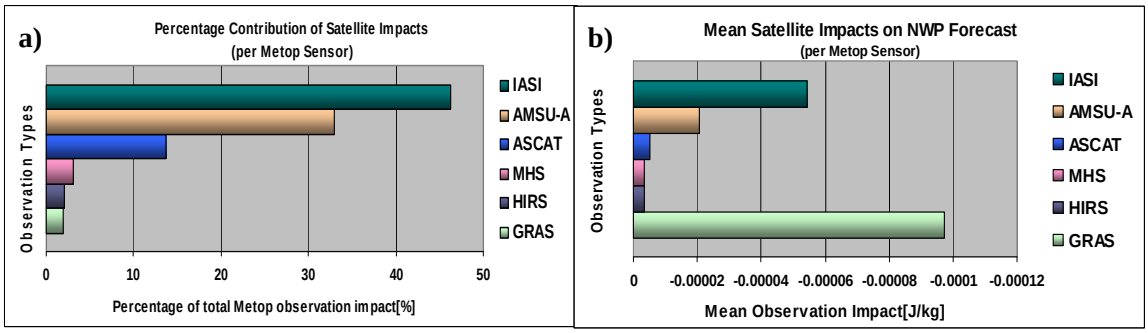

Figure 7. As in Figure 4, but for the “Metop sensor” categories described in Table 3.

4. Discussion

The observation impact of Metop data is the largest amongst all satellite categories in this study; this is despite our NOAA category including data from 5 satellites (NOAA-15

to NOAA-19). The large observation impact of Metop compared to NOAA is mainly due to the additional sensors on the platform - IASI, ASCAT and GRAS. The observation impacts by AMSU-A, MHS and HIRS on-board Metop-A are similar to those of NOAA satellites. This means that, even though AMSU-A, MHS and HIRS on-board Metop-A observe the same geographical locations as IASI, their impact on forecast error is not diminished by the additional information from IASI.

The overall observation impact of surface-based observations is smaller than that of satellite data and has become smaller following the advent of new satellite data such as IASI and AIRS. It should be stressed, however, that surface-based observations show large mean observation impacts. The observation impact per sounding for SONDE is about ten times larger than that for Metop-A in this study (not shown). Each SONDE observation has a significant impact in reducing the forecast error.

GPSRO has the largest mean observation impact among the satellite techniques in this study. The mean observation impact changes depending on the data used in a data assimilation system, and it cannot be assumed that the increased number of GPSRO data will continue to reduce the forecast error linearly; however, it can be said that GPSRO data seems to be one of the most promising satellite observing techniques for improving short-range NWP forecasts by increasing observation numbers.

This study measures the forecast error reduction in the troposphere only (from surface to 150hPa). Observations which have a strong impact on the upper atmosphere will not, therefore, be fully assessed. For example, GPSRO observes very well at levels above the troposphere. Other studies have shown stronger impact in the stratosphere than in the troposphere (Cardinali, 2009).

The Metosat AMVs have an overall strong positive observation impact in the Met Office system; however, Cardinali (2009) showed some degradation of NWP forecast accuracy due to AMVs derived from the visible and infrared frequency bands at levels below 700hPa from Meteosat in the ECMWF system. Gelaro et al. (2010), in work comparing the observation impact between the global NWP forecast systems (at NRL, GMAO and Environment Canada), noticed that the benefit of AMV data is quite different depending on the forecast system. The strong positive contribution of Meteosat AMV in the Met Office system appears to be caused by the aggregation of small contributions from a large number of observations, as described in section 3c.

5. Summary and future work

In this study, observation impacts on 24-hour forecast error reduction are evaluated using the adjoint-based Forecast Sensitivity to Observations (FSO) method developed within the Met Office NWP system. Observation impacts are produced for the period 18Z 22 August to 12Z 18 September 2010 at 6-hour intervals using the version of the NWP system that was operational at the Met Office from 16 March 2011.

Results show that satellite data accounts for 64% of short-range forecast error reduction, the remaining 36% coming from surface-based observation types. Metop-A data are measured to have the largest impact of any individual satellite platform (about 25% of the total impact on global forecast error reduction). Their dominant role, compared with NOAA satellites, is mainly due to Metop-A's additional sensors (IASI, ASCAT and GRAS). Radiosonde profiles give the largest impact among surface-based observation types, followed by aircraft, land surface and sea surface data. Even though the total impact of surface-based observations is smaller than that of satellite data, the observation impact per profile for radiosondes is about ten times larger than that for an average Metop-A sounding.

Microwave and hyper-spectral infra-red sounding systems are found to give the largest total impacts; however, GPSRO observations are measured to have the largest mean observation impact. In general it is operational satellites, rather than research satellites, which generate most forecast error reduction. The EOS-Aqua/AIRS instrument, however, was found to have an observation impact comparable with that of operational satellite sounders.

This report deals with observation impact in an average sense, assessing the overall performance of the satellite data in the context of a state-of-the-art NWP system; however, the impact of satellite data will vary depending on surface properties, cloud interactions, observing time and so on. The effects of these varying conditions are not explored in this study. As mentioned previously, adjoint-based FSO methods can measure forecast impacts for any subset of observations. We intend to use the tool to investigate further the impact of satellite data as a function of these parameters and to provide guidance to improve the use of current satellite data. We also expect results to contribute to discussions on the future development of observing systems.

Acknowledgements

The authors wish to thank Andrew Lorenc for his initial development of the adjoint-based sensitivity tools used in this study.

References

Bouttier, F., and G. Kelly, 2001: Observation-system experiments in the ECMWF 4D-Var data assimilation system. *Q. J. R. Meteorol. Soc*, **127**: 1469-1488.

Cardinali, C., 2009: Monitoring observation impact on short-range forecast. *Q. J. R. Meteorol. Soc*, **135**: 239-250.

Gelaro, R., R. H. Langland, S. Pellerin and R. Todling, 2010: The THORPEX observation impact intercomparison experiment, *Mon. Wea. Rev.*, **138**, 4009-4025.

Gelaro, R., Y. Zhu and R. M. Errico, 2007: Examination of various-order adjoint-based approximations of observation impact. *Meteor. Z.*, **16**, 685-692.

Joo, S., A. C. Lorenc and R. Marriott, 2012: Diagnosis of exaggerated impacts on adjoint-based sensitivity studies, Met Office Tech Note, In preparation.

Kelly, G., and J.-N. Thépaut, 2007. 'Evaluation of the impact of the space component of the Global Observation System through Observing System Experiments.' Pp. 16-28 in ECMWF Newsletter 113, Autumn 2007.

Langland, R. H., and N. Baker, 2004: Estimation of observation impact using the NRL atmospheric variational data assimilation adjoint system. *Tellus*, **56A**, 189–201.

Lorenc A. C. and R. Marriott, 2012. Observation impacts in the Met Office global NWP system. In preparation.

Pavelin, E. G., B. Candy and S. Joo, 2012: Assimilation of surface-sensitivity infrared radiances over land: Estimation of land surface temperature and emissivity. In preparation.

Appendix A – Glossary

AATSR Advanced Along Track Scanning Radiometer

AIREP Aircraft Report

AIRS Atmospheric Infrared Sounder

AMDAR Aircraft Meteorological Data Relay

AMI Advanced Microwave Instrument

AMSU Advanced Microwave Sounding Unit

AMV Atmospheric Motion Vector

ASCAT Advanced Scatterometer

AVHRR Advanced Very High Resolution Radiometer

BOGUS Bogus observations generated by National Meteorological Centres

CLR Clear Sky Radiance

COSMIC Constellation Observing System for Meteorology Ionosphere and Climate

DMSP Defense Meteorological Satellite Program

DROP SONDE Upper level observing device designed to be dropped from aircraft

ENVISAT Environmental Satellite

EOS Earth Observing System of NASA

ERS European Remote Sensing Satellite of ESA

ESA European Space Agency

FSO Forecast Sensitivity to Observations

GEO Geosynchronous Orbit

GMAO Global Modelling and Assimilation Office of NASA

GNSS Global Navigation Satellite System

GOES Geostationary Operational Environmental Satellite

GPS Global Positioning System

GPSRO Global Positioning System Radio Occultation

GRACE Gravity Recovery And Climate Experiment

GRAS GNSS Receiver for Atmospheric Sounding

HIRS High-resolution Infrared Radiation Sounder

IASI Infrared Atmospheric Sounding Interferometer

IR Infrared

IRS Infrared Sounder

LEO Low Earth Orbit

MHS Microwave Humidity Sounder

MODIS Moderate-resolution Imaging Spectroradiometer

MSG Meteosat Second Generation

MTSAT Multi-functional Transport Satellite

MW Microwave

MWI Microwave Imager

MWS Microwave Sounder

NASA National Aeronautics and Space Administration of the USA

NOAA National Oceanic and Atmospheric Administration of the USA

NRL Naval Research Laboratory of the USA

NWP Numerical Weather Prediction

OSE Observing System Experiment

PILOT Upper level wind observation

SCAT Scatterometer

SEVIRI Spinning Enhanced Visible and Infrared Imager

SFC Surface

SHIP Sea surface weather observation by ship

SSMI Special Sensor Microwave Imager

SSMIS Special Sensor Microwave Imager/Sounder

SST Sea Surface Temperature

SYNOP Land surface synoptic weather observations

TEMP Upper level pressure, temperature, humidity and wind observation

TCBOGUS Tropical Cyclone Bogus

WINDSAT Wind Satellite

Met Office
FitzRoy Road, Exeter
Devon EX1 3PB
United Kingdom

Tel (UK): 0870 900 0100 (Int) : +44 1392 885680
Fax (UK): 0870 900 5050 (Int) :+44 1392 885681
enquiries@metoffice.gov.uk
www.metoffice.gov.uk